Paramagnetic salt pill design for magnetic refrigerators used in space applications

C. Hagmann, D.J. Benford and P.L. Richards

Department of Physics and Space Sciences Laboratory, University of California, Berkeley, CA 94720, USA

Received 9 August 1993; revised 9 September 1993

An adiabatic demagnetization refrigerator (ADR) is described which was designed for use in the multiband imaging photometer for the Space Infrared Telescope Facility (SIRTF). This refrigerator was required to cool bolometric detectors for infrared and millimetre waves to 0.1 K. A paramagnetic salt pill with a number of novel features was developed to meet the stringent requirements for an ADR used in space. An unusual paramagnetic salt, chromic caesium alum (CCA), is used to meet the requirement of thermal stability under the bake-out temperatures used in commissioning space cryogenic vacuum systems. The cycle time for the refrigerator has been reduced to ≈30 min by attention to thermal time constants and by growing the CCA salt directly on to an array of gold wires. Crystal growing procedures were developed to overcome problems with the low solubility of CCA in water. The salt pill is sealed in stainless steel to retain water of hydration and is constructed of materials which are not corroded by commonly used paramagnetic salts.

Keywords: adiabatic demagnetization; refrigerators; space cryogenics

Interest in the application of adiabatic demagnetization refrigerators (ADRs) to the cooling of bolometric detectors for astronomical observations has grown rapidly in recent years. Temperatures below 100 mK can be reached starting from a superfluid helium reservoir at 1.5–2 K. Under usual circumstances, the power dissipation in the detectors is negligible, and efficient lightweight single shot refrigerators can be built with a hold time of more than 24 h and a duty cycle of 95%. The efficiency of such refrigerators is close to thermodynamic limits. They do not require the containment of cryogenic fluids and operate naturally in zero *g*. Most issues of space qualification can be met in a straightforward way.

The salt pill technology described in this paper was developed for use on a specific space mission. The Space Infrared Telescope Facility (SIRTF)[1] is a proposed NASA satellite observatory which was designed to study astronomical sources in the wavelength range from 1.8 to 1200 μm. The observatory will be cooled by superfluid helium and will feature three instruments: the infrared array camera (IRAC), the infrared spectrometer (IRS) and the multiband imaging photometer for SIRTF (MIPS). The MIPS will have arrays of detectors and will operate in both diffraction limited and wide field modes. Bolometers were proposed for wavelengths between 200 and 1500 μm. To achieve background and confusion limited sensitivity, the bolometers must have a noise equivalent power (NEP) $\leq 2 \times 10^{-17}$ W Hz$^{1/2}$. This sensitivity requires cooling to temperatures below those attainable by ^{3}He refrigerators. The MIPS project proposed to use bolometers cooled to 0.1 K by an ADR. The prototype SIRTF refrigerator is described in Timbie *et al.*[2]. A summary of the SIRTF ADR project will be published at a later date[3].

In the spring of 1992, rationalization due to budgetary constraints forced removal of the long wavelength bolometric channels from the MIPS. Consequently, it does not appear that the technology described here will be flown in its intended mission. However, an ADR with very similar requirements is required to cool X-ray bolometers on the approved NASA AXAF spacecraft[4–6]. Also, use of ADRs to cool infrared bolometers is being discussed for the NASA Submillimeter Moderate Mission and the FIRST project of the European Space Agency. On a shorter term, ADR technology has been used successfully to cool infrared bolometers for measurement of the anisotropy of the cosmic microwave background on a balloon telescope[7,8] and from the South Pole[9] and plans are well advanced to cool X-ray bolometers on a sounding rocket[10]. It is anticipated that many of the developments described here will be useful for a variety of

0011–2275/94/030213–07

future missions. In addition, ADRs similar to the one described here are being used as quick turnaround test facilities for the development of detectors for millimetre waves, X-rays and dark matter particles.

Principles of adiabatic demagnetization

Refrigeration by adiabatic demagnetization relies on the dependence of the entropy $S(T, B)$ of the magnetic dipoles in a paramagnetic material on magnetic field and temperature. Extensive discussions of this process may be found in the literature[11–13]. The magnetic entropy of actual paramagnetic materials can be described in a semiquantitative way by reference to the entropy calculated for an ideal paramagnet consisting of n non-interacting moments per unit volume, each characterized by a quantum number J

$$S(T, B) = nk\left[\ln\left(\frac{\sinh[(2J+1)x/2]}{\sinh[x/2]}\right) + x/2\coth x/2 - (2J+1)x/2\coth(2J+1)x/2\right] \quad (1)$$

where $x = g\beta B/kT$, $\beta = 9.27\times10^{-24}\,\mathrm{J\,T^{-1}}$ is the Bohr magneton and $k = 1.38\times10^{-23}\,\mathrm{J\,K^{-1}}$ is Boltzmann's constant.

The Landé factor g depends on the paramagnetic material. For paramagnetic salts containing elements of the iron group, g is close to the free spin value of 2 and is isotropic. In some rare earth compounds, on the other hand, g differs greatly from 2 and is strongly anisotropic. Examples of the latter cases are the paramagnets caesium magnesium nitrate and dysprosium gallium garnet, commonly referred to as CMN and DGG.

The function $S(T, B)$ is plotted for the case $g = 2$ in *Figure 1* for several values of J. For this ideal paramagnet, the magnetic entropy in zero field has the constant value $S = nk\ln(2J+1)$ at all temperatures. In real paramagnets, interactions between the magnetic moments themselves and/or the crystal field will split the zero field degeneracy, resulting in a vanishing entropy at zero temperature as required by the third law of thermodynamics. Typically, these interactions become important at temperatures slightly above the transition temperature at which the salt enters an ordered magnetic phase. Therefore, the transition temperatures give an estimate of the lowest temperature obtainable by demagnetization of a particular paramagnetic material. Equation (1) is still approximately valid for temperatures $\gtrsim T_{int}$ if we represent the internal interactions by a fictitious internal field $B_{int} = kT_{int}/2Jg\beta$ and replace B in Equation (1) by $(B^2 + B_{int}^2)^{1/2}$.

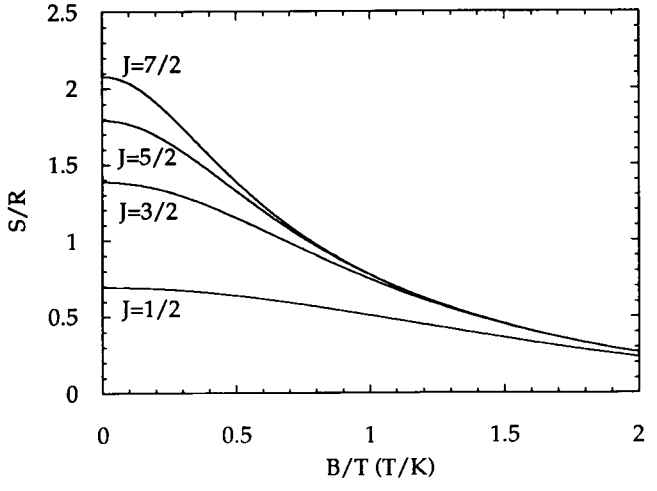

Figure 1 Magnetic entropy of ideal paramagnet for various values of J and $g = 2$

Thus our estimate of the magnetic entropy of a real material in zero external field is given by $S(T, B_{int})$ from Equation (1). From this simple viewpoint, each material is characterized by three parameters, n, J and B_{int}. For most candidate materials, the number of moments per unit volume n is known from the chemical formula and the crystal structure. The magnetic moment quantum number is also generally known from the magnetic ion and the site symmetry. The effective internal field B_{int} can be estimated qualitatively from the magnetic ordering temperature, or more quantitatively from low temperature measurements of magnetic entropy.

The refrigeration cycle can be illustrated by reference to the S–T diagram[14,15] of the paramagnetic material chromic caesium alum (CCA) shown in *Figure 2*. The cycle begins at point A, at which the salt pill is thermally connected to the high temperature reservoir at temperature T_i by a heat switch. The magnetic entropy at this point is essentially $S = nk\ln(2J+1)$ per moment. The salt pill is then isothermally magnetized from zero applied field to the maximum field of the magnet at point B. During this process, the spins become aligned in the field direction and the entropy of the salt is reduced by ΔS. The heat of magnetization, corresponding to $\Delta Q = T_i\Delta S$, is transferred to the reservoir. The thermal contact to the reservoir is then broken and the applied field is reduced adiabatically along the path B → C. If the external field is reduced to zero, the final temperature is determined by the intersection with the curve for $B = 0$, which depends on the effective internal B_{int}. Heat leaking into the salt pill along supports or electrical connections then warms up the system along the $B = 0$ curve.

It is possible to maintain a detector at a constant temperature by partially isolating it from the salt pill and heating it to the desired temperature. The amount of heat that the pill can absorb during this process is represented by the area to the left of the $B = 0$ curve. A more efficient way to obtain a stable detector temperature is called isothermal demagnetization. In this cycle, illustrated in *Figure 2*, the salt pill is demagnetized adiabatically to the point C where the desired operating temperature T_f is reached. The field is then reduced slowly along the path C → D as required to compensate for the heat leak. During this isothermal demagnetization, the salt can absorb an amount of heat given by $T_f\Delta S$, which is the shaded area to the left of the line C → D. The entropy difference per unit mass of salt determines the time that the refrigerator will operate between cycles. It can be maximized by choosing a salt with an ordering temperature sufficiently below the desired operating temperature that $S(T_f, B_{int})$ is close to its high temperature limit, but also with a large J and large n per unit mass. Since the

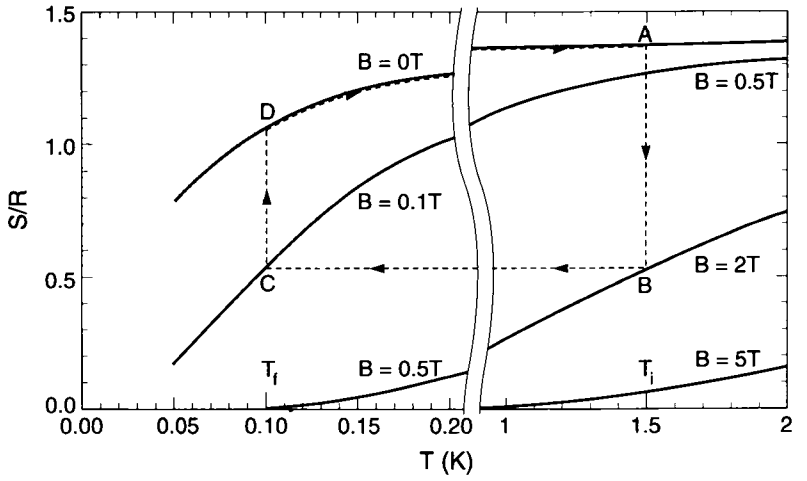

Figure 2 Entropy of CCA in a magnetic field calculated assuming two doublets with a Stark splitting of 191 mK. The approximation breaks down near the ordering termperature $T = 10$ mK. The lattice entropy is negligible below ≈2 K

value of B_{int} increases with n and J, a compromise is necessary. In practice, a salt is chosen with a sufficiently small value of B_{int} for which the values of n and J are as large as possible.

Choice of paramagnet

The operating temperature of the SIRTF ADR was chosen to be $T_f = 100$ mK in order to meet the requirement that the observations be background limited. The paramagnetic materials commonly used for this temperature range are hydrated salts containing elements from the iron group. Two popular salts are ferric ammonium alum (FAA) with $J = 5/2$ and chromic potassium alum (CPA) with $J = 3/2$. The dipole–dipole and exchange interactions in these compounds are small due to the relatively large spacing between magnetic ions. The effective internal magnetic field is ≈50 mT for FAA and ≈20 mT for CPA. A disadvantage of the alums is their tendency to dehydrate at room temperature. This problem is usually countered by coating the crystals with varnish or sealing them in a vacuum-tight container. Much effort has been made to find different materials with low magnetic ordering temperatures which are stable at room temperature. Some examples of candidate materials are Cr^{3+} doped Al_2O_3 (synthetic ruby) and Er^{3+} or Nd^{3+} substituted YAG. However, the degree of dilution required to achieve a low ordering temperature results in a small entropy density and a smaller cooling capacity than can be obtained from the alums. It was therefore decided to use an alum in the SIRTF ADR but one with better thermal stability than CPA or FAA.

Since the SIRTF cryostat is likely to be baked before cooling, the thermal stability of its components is a major concern. The size of the non-magnetic cation in the chromic alums influences the bonding strengths of the waters of hydration. The water vapour pressure decreases monotonically with increasing cation size for fixed temperature. In this work, CCA was shown to resist dehydration at room temperature and to withstand temperatures above 50°C without damage when in a sealed container. The chemical formula of this alum is $CsCr(SO_4)_2 \cdot 12H_2O$ which is the same as for CPA with caesium substituted for potassium. Crystals of CCA are dark violet in colour and have a density of 2.06 g cm^{-3}. Its low temperature magnetic properties are similar to those of CPA. The Landé factor g is isotropic and ≈2 and $J = 3/2$. The lowest degenerate quadruplet is split into two Kramers doublets with $\delta =$ 191 mK by the crystal field[14,15]. The remaining degeneracy is lifted by magnetic and exchange interactions with an ordering temperature of ≈10 mK.

Salt pill construction

A satisfactory design for the salt pill must solve problems of mechanical support, thermal contact to the salt, protection of metal parts from corrosion, prevention of dehydration of the salt and avoidance of excessive eddy current heating during demagnetization.

Several techniques have been used to obtain good thermal contact to the salt. In one, crystalline slabs of the salt are glued between layers of coil-foil (varnished mats of fine copper wire). Another method is to compress powdered salt with embedded wires or vanes in a die. In the AXAF ADR, FAA crystals are grown out of an aqueous solution on an array of gold-plated copper wafers[6]. We crystallize the CCA salt directly onto a mesh of 200 gold wires 0.25 mm in diameter. Gold is used for its high thermal conductivity and to resist corrosion. The cost of the 25 g of gold is not prohibitive compared with the total cost of producing the salt pill. The wires are held in a 1.5 mm triangular lattice by two Teflon spacers located at each end of the salt pill, as shown in *Figure 3*. The bundle of wires passes through a hole in a stainless steel cap and fills a 4 cm deep axial hole in the OFHC copper bolt, which serves as the thermal bus to the bolometers. Silver solder is used to fill the small gap between the wires and the bolt. Solder is also flowed into a small cup at the

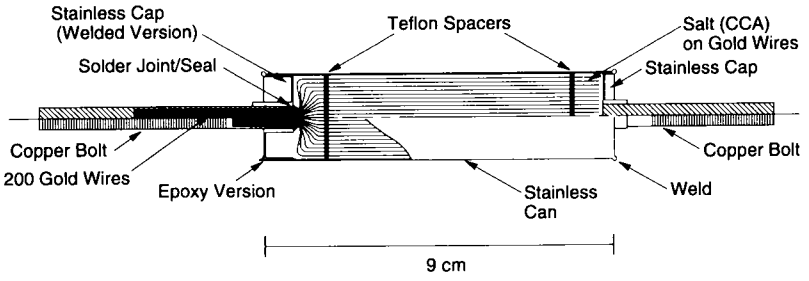

Figure 3 Salt pill shown in cross-section on the left and external view on the right

interface between the gold wires and the stainless cap. The solder joint is afterwards gold plated or coated with epoxy to protect it from corrosion. In this way, the thermal resistance of the solder is minimized and the only materials to contact the salt are gold, stainless steel and epoxy, none of which is attacked significantly by any of the alums. Cadmium-rich silver solder[16] which becomes superconducting at temperatures below 100 mK has been used in salt pills but can result in trapping of magnetic flux, preventing complete demagnetization. The silver solder used in this work (Eutecrod 1800, Eutectic Corp., NY, USA) contains no cadmium.

The copper bolt is threaded and electroplated with 25 μm of gold to resist oxidation. Mechanical and thermal contact to the cold stage is made by clamping it to the bolt between two gold plated copper nuts. A second threaded copper bolt is attached at the opposite end of the pill. The two copper bolts are used to suspend the 100 mK stage from the 1.5 K cold plate by means of tensioned Kevlar cords[2].

The salt pill is surrounded by a can made of nominally non-magnetic 304 stainless steel to protect it from dehydration in a vacuum. Stainless steel is used because of its resistance to corrosion, its mechanical strength and its poor electrical conductivity. Stainless steel has a relatively large electronic heat capacity and cooling it down to ADR operating temperatures leads to a loss in available entropy $\Delta S = \int (C/T)\,dT$ of the overall cold stage. In our design, we use about 20 g of stainless steel and thereby lose $\approx$3% of cooling capacity at 100 mK.

The can consists of a 250 μm thick tube with two end caps. The end cap opposite to the gold wires was argon arc welded to the tube before assembly. Two designs have been used for the other end cap. One is designed to be welded to the walls after assembly to provide a reliable seal for space applications. Important features of the design include the absence of contact between the salt and the end cap and the extended side wall on the end cap shown in *Figure 3*. Welding has been successfully accomplished by taking care to heat sink the side walls and the copper bolt. In a test weld completed in 30 s, the temperature rise in the salt close to the end cap was measured to be $\approx$5°C. The second design consists of an epoxy seal (Stycast 2850 FT, Emerson and Cumings, MA, USA) to an inverted end cap, also shown in *Figure 3*. This approach proved convenient during the experimental development.

Attention was given to sources of eddy current heating. The power dissipation in a cylinder of length L, radius R and resistivity ρ and with the axis parallel to the magnetic field is

$$P_{eddy} = \pi \dot{B}^2 R^4 L/8\rho \qquad (2)$$

In our design the dominant losses occur in the copper bolts. Assuming a ramp rate of 1 T min^{-1}, the estimated eddy current power is $\approx 1\,\mu$W. By contrast, the eddy current power of the stainless parts calculated from the radial derivative of Equation (2) is $\approx 0.03\,\mu$W, while the gold wires contribute $\approx 0.002\,\mu$W.

Salt pill growth

Growing crystals from solution requires that the solution be supersaturated. This can be done by reduction of the water content in the solution by evaporation or by reducing the solubility of the salt by cooling. We have adopted the latter method. A schematic diagram of the growing apparatus is shown in *Figure 4*. The salt pill skeleton is held in a Lucite mould consisting of two blocks which, when bolted together, leave a circular hole the diameter of the desired salt pill. A narrow channel is cut into each block to allow solution to flow around the Teflon spacers. Small amounts of silicone rubber are applied to the joints to make a water-tight seal. The copper bolt and attached gold wires are cooled by thermoelectric coolers

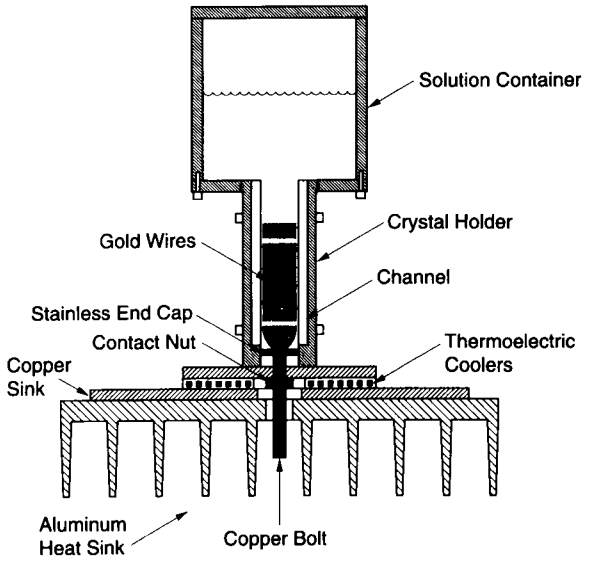

Figure 4 Growing apparatus for CCA salt pills

(DT 1089–13, Marlow Industries, TX, USA) to encourage the preferential growth of crystals on the wires. The temperature of the bolt is maintained near 0°C. The heat generated by the coolers is rejected into an aluminium heat sink cooled by a fan. A Lucite container containing saturated solution is mounted on top of the mould.

The speed of growth is largely determined by the solubility of the salt. The solubility of CCA in water is $9.6\,g\,dm^{-3}$ at $T = 25°C$, compared to $244\,g\,dm^{-3}$ for CPA and $1244\,g\,dm^{-3}$ for FAA[17], as is shown in *Figure 5a*. The solubility of CCA can be greatly increased by adding nitric acid[18], as shown in *Figure 5b*. Using 20% of HNO_3 by weight leads to a 13-fold increase in solubility with no change in the composition of the crystal. Since CCA is not commercially available, we obtain it by combining equivalent amounts of the component salts Cs_2SO_4 and $Cr_2(SO_4)_3 \cdot 12H_2O$. It is important to use the hydrated violet form of chromium sulfate (Johnson–Matthey, MA, USA) for this purpose and not the dehydrated greenish form. The saturated solution at 25°C is mixed with a magnetic stirrer and poured into the growing apparatus and allowed to cool. Depending on the amount of solution in the container it is necessary to exchange the depleted solution with fresh saturated solution. The crystals grow readily around the gold wires reaching a typical size of a few millimetres, which is comparable to the wire spacing. No damage to the crystals was observed after repeated cycles between room temperature and $T = 77\,K$. A large crystal size improves the thermal conductivity of the salt at low temperatures which is limited by the grain size. Typically, the growth of a 40 g (0.07 mole) CCA pill requires two weeks.

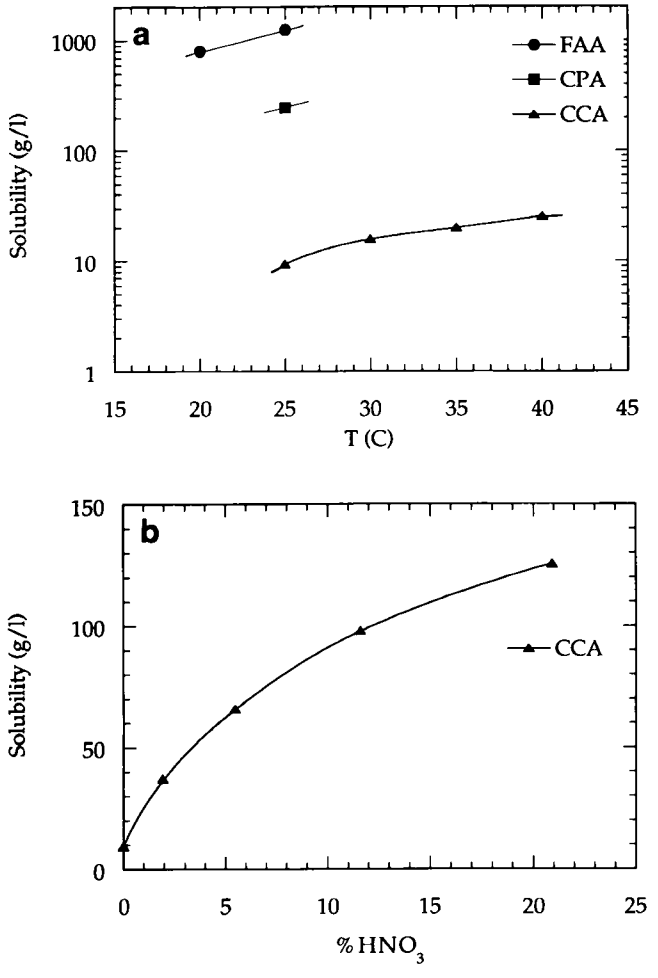

Figure 5 (a) Temperature dependence of solubility of CCA compared with that of FAA and CPA. (b) Solubility of CCA as a function of HNO_3 concentration at $T = 25°C$

The growth procedure for FAA pills is simpler due to the large solubility of FAA. The solution container shown in *Figure 4* is not used. The Lucite mould is filled with saturated FAA solution at room temperature. It is then cooled to ≈10°C for one day in a refrigerator. The mould is then opened and unwanted crystals are removed. This cycle is repeated a few times until a filling fraction of ≈90% has been reached.

Bake tests

Large cryostats, including those used on spacecraft, are usually baked to reduce the pump-out time. The temperature is limited by the possibility of damage to sensitive components. In infrared spacecraft, for example, indium bump bonded detector arrays are particularly heat sensitive. The COBE Dewar was baked at 10°C above ambient which reduced the pump time by a factor of two[19]. To be useful in most space applications, a salt pill must survive this bake-out. The maximum temperature which a salt can survive is indicated by its melting point. FAA melts at 40°C, CPA at 89°C and CCA at 116°C. Dehydration of the crystals, however, typically starts at much lower temperatures. Two CPA pills have been tested[20] at NASA/Ames after baking for two weeks at 50 and 70°C, respectively. The refrigerator was able to reach 0.1 K using a pill baked at 50°C, but only a lower limit for the cooling capacity was quoted. The performance of the pill baked at 70°C was seriously degraded.

Bake tests of CCA were made by sealing crystals in vacuum-tight vials to contain the water of hydration and placing them in a temperature-regulated oven. After baking, the crystals were removed from the vials and visually inspected for damage. Dehydrated salt is greenish in colour and was easily identified. It was scraped off and weighed. We baked several containers which were 10% full of CCA at 55°C for six weeks. The average fractional degradation was determined to be 1%. The equilibrium water vapour pressure[17] of CCA of ≈38 torr * at this temperature could be reached if 1% of the CAA molecules each gives off a single H_2O molecule. A second bake test at 50°C for two weeks with a 20% filling fraction yielded no observable degradation. We therefore conclude that the sealed CCA salt pill developed here can withstand a bake-out temperature of 50°C for at least two weeks.

Thermal characteristics

The thermal contact between the paramagnetic salt and the cold stage is a major factor in the efficiency of the ADR. It is desirable to avoid large thermal gradients

* 1 torr = 133.322 N m^{-2}

during demagnetization which cause irreversible heat flows and an increase of the entropy of the pill. Furthermore, short thermal time constants are beneficial for active temperature stabilization at low temperature. Finally, a good thermal design minimizes the time for isothermal magnetization and maximizes the duty cycle of the ADR.

The time constant for reaching equilibrium within the salt increases rapidly with decreasing temperature. We use wires inside the salt to reduce the distances over which heat flows in the salt and to increase the contact area between metal and salt. The thermal conductivities of the metal parts are proportional to T whereas the conductivity of the salt varies as T^3. Moreover, at temperatures below about 100 mK, the thermal boundary resistance at the salt–gold interface becomes important. The boundary resistance between varnished copper and CPA has been measured to be[21]

$$R_b = \Delta T/P \simeq 30/AT^3 \ (\mathrm{K^4\,cm^2\,W^{-1}}) \qquad (3)$$

where A is the boundary area and P the power flowing across the interface. The theoretical value for R_b at the interface between gold and CPA is[22] $17/AT^3\,(\mathrm{K^4\,cm^2\,W^{-1}})$. Values for the interface between gold and other alums are expected to be similar.

Only limited amounts of thermal conductivity data are available for the alums. The conductivity of single crystal CPA has been measured[23] near $T = 0.2$ K to be $K \approx 0.05\,\mathrm{T^3\,W\,cm^{-1}\,K^{-1}}$. The conductivity of polycrystalline samples is expected to be even smaller at low temperatures since the conductivity is then limited by boundary scattering. In this limit, it has been estimated[12] that $K \approx D\ \mathrm{T^3\,W\,cm^{-1}\,K^{-1}}$, where D is the grain diameter in cm.

Table 1 lists the thermal conductivities and heat capacities at $T = 100$ mK of the materials used in the salt pill. The salt occupies a volume of $\approx 30\,\mathrm{cm^3}$ and contributes most of the heat capacity of the pill. *Table 2* contains estimates of the thermal resistances of various parts of the thermal bus. Since the resistance down the length of the salt is 100 times larger than the resistance down the gold wires, the heat will flow predominantly between the salt and nearest wire and along the wires. A power input P into the 100 mK stage will set up a temperature gradient with $\Delta T = PR$ where the resistance of the gold wires dominates the total R. Our ADR has a heat leak of $\approx 0.25\,\mu$W and will therefore have a $\Delta T = 0.25$ mK.

The thermal time constant of the 100 mK stage depends on the heat capacity of the addenda. The time constant of two stages with heat capacities C_1, C_2 connected by a thermal resistance R is $\tau = C_1C_2R/(C_1 + C_2)$, assuming that internal time constants can be neglected. For example, if $C_1 = 0.2\,\mathrm{J\,K^{-1}}$ is the capacity of the salt and $C_2 = 2.5 \times 10^{-4}\,\mathrm{J\,K^{-1}}$ is due to 200 g of copper and $R = 1000\,\mathrm{K\,W^{-1}}$ is the resistance of the gold wires, we obtain $\tau = C_2R = 200$ ms. By contrast, the internal time constant $\tau_{int} \approx C_1R = 200$ s of the salt pill is considerably longer. However, in regulation mode at a constant temperature, the salt is approximately isothermal (provided the magnetic field is homogeneous) and the effective time constant is much smaller. These time constants could be reduced if desired by increasing the number or diameter of the gold wires.

Table 1 Thermal conductivities and heat capacities of salt pill components at $T = 100$ mK. The experimental values of residual resistivity ratio (*RRR*) for the metals between 4.2 and 300 K are shown

Component	κ (W K^{-1} cm^{-1})	C (J K^{-1} cm^{-3})	Comments
CPA[23,24]	5×10^{-5}	7.2×10^{-3}	$B = 0$
Au[25,26]	1.2×10^{-1}	7.3×10^{-6}	*RRR* = 146
Cu[21,26]	1.1×10^{-1}	1.0×10^{-5}	*RRR* = 88
Stainless steel[11,27]	1×10^{-4}	3.6×10^{-4}	Heat capacity extrapolated from $T = 1$ K

Table 2 Estimated thermal resistances of salt pill components at $T = 100$ mK

Component	R(K W^{-1})	Comments
Cu bolt	140	$L = 5$ cm $R = 0.32$ cm
Au wires	830	$L = 10$ cm $R = 1.25 \times 10^{-2}$ cm, 200 wires
Au–salt boundary	140	$A = 1.25 \times 10^2$ cm^2 $R_b = 17/AT^3$ (K^4 cm^2 W^{-1})
Silver solder	10	$A = 5$ cm^2 $L = 5 \times 10^{-3}$ cm
Salt	5	Radial heat flow $r1 = 0.013$ cm $r2 = 0.07$ cm

Summary of performance

The measured cooling capacity of our salt pills is close to theoretical expectations. The amount of heat the salt pill can absorb at T_f is $\Delta Q = T_f \Delta S = T_f[S(B_i, T_i) - S(0, T_f)]$. For $T_i = 1.6$ K, $T_f = 0.1$ K, $B_i = 2$ T and a salt pill containing 0.065 mole of CCA, the calculated cooling capacity $\Delta Q = 26$ mJ. The measured cooling capacity at 100 mK was ≈ 24 mJ. The difference can be attributed to the fact that the magnetic field falls off towards the ends of the pill. For a typical heat leak of $\approx 0.25\,\mu$W, the ADR hold time is about 26 h.

The durability of the salt pills is a major concern. Among about eight salt pills produced over the last few years, one FAA pill failed after many thermal cycles between room temperature and liquid helium temperature because of a leak in the epoxy joint. The flight versions of our pill are designed to be welded shut. Because of the termination of the SIRTF project, not all of the tests required to demonstrate the space worthiness of our CCA pills have been carried out. Since the salt is not rigidly constrained inside the can, there is some concern that it could be damaged by launch vibration. Vibration tests at 77 K are planned and will be carried out when the opportunity arises. It is possible that a filler will be required to improve the mechanical support.

Conclusions

We have successfully tested a novel salt material (CCA) and shown that it is well-suited for demanding

space applications. We have designed and produced reliable and efficient salt pills for use in ADRs to cool IR and X-ray detectors. For less critical applications the same design is usable with the common materials FAA and CPA.

Acknowledgement

This work was supported by NASA Grants FD-NAGW-2121 and NAGW-2864.

References

1 **Rieke, G.H., Lada, C., Lebofsky, M., Low, F. *et al.*** Instrumentation for optical remote sensing from space *Proc Soc Photo-Opt Instrum Eng* (1985) **589** 242
2 **Timbie, P.T., Bernstein, C.M. and Richards, P.L.** Development of an adiabatic demagnetization refrigerator for SIRTF *Cryogenics* (1990) **30** 271–275
3 **Hagmann, C., Timbie, P. and Richards, P.L.** manuscript in preparation
4 **Serlemitsos, A., Warner, B., Castles, S., Breon, S. *et al.*** Adiabatic demagnetization refrigerator for space use *Adv Cryog Eng* (1990) **35** 1431–1437
5 **Serlemitsos, A., SanSebastian, M. and Kunes, E.** The AXAF/XRS ADR: Engineering model *Adv Cryog Eng* (1992) **37** 899–905
6 **Serlemitsos, A., SanSebastian, M. and Kunes, E.** Design of a spaceworthy adiabatic demagnetization refrigerator *Cryogenics* (1992) **32** 117–121
7 **Fischer, M.L., Alsop, D.C., Cheng, E.S., Clapp, A.C. *et al.*** A bolometric millimeter-wave system for observations of anisotropy in the cosmic microwave background radiation on medium angular scales *Astrophys J* (1992) **388** 242–252
8 **Alsop, D.C., Cheng, E.S., Clapp, A.C., Cottingham, D.A. *et al.*** A search for anisotropy in the cosmic microwave background on intermediate angular scales *Astrophys J* (1992) **395** 317–325
9 **Ruhl, J. and Dragovan, M.** A sportable 0.05 K refrigerator for astrophysical observations *Proc 4th Int Workshop on Low Temperature Detectors for Neutrinos and Dark Matter* (Eds Booth, N.E. and Salmon, G.L.) Edition Frontiers, Gif sur Yvette, France (1991) 461–464
10 **McCammon, D.** personal communication, University of Wisconsin, USA (1993)
11 **Lounasmaa, O.V.** *Experimental Principles and Methods Below 1 K* Academic Press, London, UK (1974)
12 **Betts, D.S.** *Refrigeratio and Thermometry Below One Kelvin* Sussex University Press, UK (1976)
13 **Hudson, R.P.** *Principles and Applications of Magnetic Cooling* North-Holland, Amsterdam, The Netherlands (1972)
14 **Bleaney, B.** Paramagnetic resonance spectra of five chromic sulphate alums at low temperatures *Proc Roy Soc* (1950) **A204** 203–216
15 **Hudson, R.P.** Properties of the Cr^{+++} ion in the paramagnetic alums at low temperatures *Phys Rev* (1952) **88**(3) 570–572
16 **Landau, J. and Rosenbaum, R.** Superconducting transition of a silver solder alloy at very low temperatures *Rev Sci Instrum* (1972) **43** 1540
17 *Gmelin's Handbook of Inorganic Chemistry* Vols 52 and 59B, Gmelin Institute for Inorganic Chemistry, Frankfurt, Germany
18 **Krauss, D.L. and Nutting, G.C.** Absorption spectra of the chrome alums at low temperatures *J Chem Phys* (1941) **9** 133–145
19 **Volz, S.M. and Ryschkewitsch, M.G.** Ground and early on-orbit performance of the superfluid helium dewar of the Cosmic Background Explorer (COBE) *Superfluid Helium Heat Transfer* Vol 134 (Eds Kelly, J.P. and Schneider, W.J.) The American Society of Mechanical Engineers, Seattle, USA (1990) 23–27
20 **Savage, M.L., Kittel, P. and Roellig, T.** Salt materials testing for a spacecraft adiabatic demagnetization refrigerator *Adv Cryog Eng* (1990) **35** 1439–1446
21 **Suomi, M., Anderson, A.C. and Holmström, B.** Heat transfer below 0.2 K *Physica* (1968) **38** 67–80
22 **Little, W.A.** The transport of heat between two dissimilar solids at low temperatures *Can J Phys* (1959) **37** 334–349
23 **Garrett, C.G.B.** The thermal conductivity of potassium chrome alum at temperatures below one degree absolute *Phil Mag* (1950) 7(41) 621–630
24 **Vilches, O.E. and Wheatley, J.C.** Measurements of the specific heats of three magnetic salts at low temperatures *Phys Rev* (1966) **148** 509–516
25 **Sharma, J.K.N.** Heat conductivities below 1 K *Cryogenics* (1967) **7** 141–156
26 **du Chatenier, F.J.** Heat capacities of some dilute alloys *Physica* (1962) **28** 181–182
27 **du Chaterier, F.J., Boerstoel, B.M. and de Nobel, J.** Specific heat capacity of stainless steel *Physica* (1965) **31** 1061–1062